AD-A088 179 ILLINOIS UNIV AT URBANA-CHAMPAIGN ELECTROMAGNETICS LAB F/G 20/14
RADIATION FROM AN OPEN-ENDED WAVEGUIDE WITH BEAM EQUALIZER, A S--ETC(U)
JUL 80 W L KO, R MITTRA, S W LEE N00014-75-C-0293
UNCLASSIFIED UIEM-80-6 NL

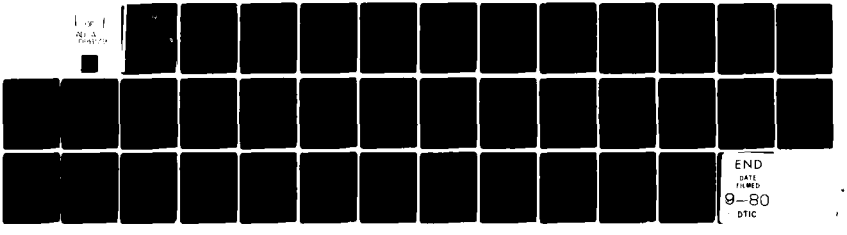

END
DATE FILMED
9-80
DTIC

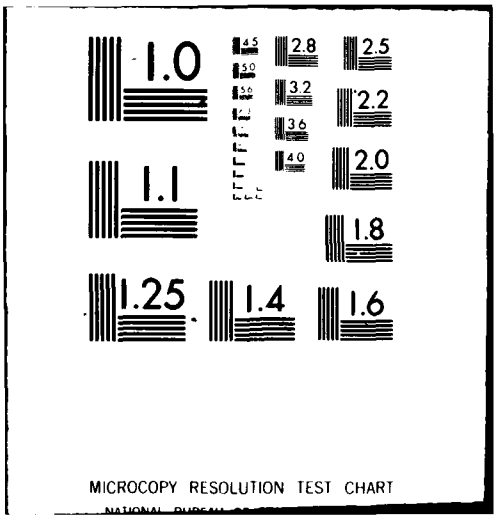
1.0
1.1
1.25
1.4
1.6
1.8
2.0
2.2
2.5
2.8
3.2
3.6
4.0
4.5
5.0
5.6
MICROCOPY RESOLUTION TEST CHART

ELECTROMAGNETICS LABORATORY
TECHNICAL REPORT NO. 80-6

July 1980

LEVEL II

RADIATION FROM AN OPEN-ENDED WAVEGUIDE WITH BEAM EQUALIZER - A SPECTRAL DOMAIN ANALYSIS

Technical Report

W. L. Ko

R. Mittra

S. W. Lee

ELECTROMAGNETICS LABORATORY
DEPARTMENT OF ELECTRICAL ENGINEERING
ENGINEERING EXPERIMENT STATION
UNIVERSITY OF ILLINOIS AT URBANA-CHAMPAIGN
URBANA, ILLINOIS 61801

Supported by
Contract No. N00014-75-C-0293
Office of Naval Research
Department of the Navy
Arlington, Virginia 22217

UNCLASSIFIED

SECURITY CLASSIFICATION OF THIS PAGE (When Data Entered)

REPORT DOCUMENTATION PAGE	READ INSTRUCTIONS BEFORE COMPLETING FORM
1. REPORT NUMBER	2. GOVT ACCESSION NO. AD-A088 179 / 3. RECIPIENT'S CATALOG NUMBER
4. TITLE (and Subtitle) RADIATION FROM AN OPEN-ENDED WAVEGUIDE WITH BEAM EQUALIZER - A SPECTRAL DOMAIN ANALYSIS.	5. TYPE OF REPORT & PERIOD COVERED TECHNICAL REPORT.
	6. PERFORMING ORG. REPORT NUMBER (14) UILU-ENG-80-2547 / EM-80-6
7. AUTHOR(s) (10) W. L. Ko, R. Mittra, and S. W. Lee	8. CONTRACT OR GRANT NUMBER(s) N00014-75-C-0293
9. PERFORMING ORGANIZATION NAME AND ADDRESS Electromagnetics Laboratory Department of Electrical Engineering University of Illinois, Urbana, IL 61801	10. PROGRAM ELEMENT, PROJECT, TASK AREA & WORK UNIT NUMBERS
11. CONTROLLING OFFICE NAME AND ADDRESS Office of Naval Research Department of the Navy Arlington, Virginia 22217	12. REPORT DATE July 1980 (11)
	13. NUMBER OF PAGES 38
14. MONITORING AGENCY NAME & ADDRESS (if different from Controlling Office) (12) 38	15. SECURITY CLASS. (of this report) UNCLASSIFIED
	15a. DECLASSIFICATION/DOWNGRADING SCHEDULE

16. DISTRIBUTION STATEMENT (of this Report)

Distribution Unlimited. Reproduction in whole or in part is permitted for any purpose of the United States Government.

17. DISTRIBUTION STATEMENT (of the abstract entered in Block 20, if different from Report)

18. SUPPLEMENTARY NOTES

19. KEY WORDS (Continue on reverse side if necessary and identify by block number)

beam equalizer; radiation; open-ended waveguide; spectral domain analysis

20. ABSTRACT (Continue on reverse side if necessary and identify by block number)

A septum and an impedance matching post are used as a beam equalizer in an open-ended waveguide-feed for reflectors used in satellite communications systems. The performance of this design over a frequency band is evaluated using a spectral domain approach. The computed radiation patterns in the E- and H-planes, as well as the results for the impedance match, are presented in the paper.

DD FORM 1 JAN 73 1473 EDITION OF 1 NOV 65 IS OBSOLETE

S/N 0102-014-6601

UNCLASSIFIED

SECURITY CLASSIFICATION OF THIS PAGE (When Data Entered)

UILU-ENG-80-2547

Electromagnetics Laboratory Report No. 80-6

RADIATION FROM AN OPEN-ENDED WAVEGUIDE WITH BEAM EQUALIZER - A SPECTRAL DOMAIN ANALYSIS

Technical Report

W. L. Ko
R. Mittra
S. W. Lee

July 1980

Office of Naval Research
Department of the Navy
Arlington, Virginia 22217

Contract No. N00014-75-C-0293

Electromagnetics Laboratory
Department of Electrical Engineering
Engineering Experiment Station
University of Illinois at Urbana-Champaign
Urbana, Illinois 61801

ABSTRACT

A septum and an impedance matching post are used as a beam equalizer in an open-ended waveguide-feed for reflectors used in satellite communications systems. The performance of this design over a frequency band is evaluated using a spectral domain approach. The computed radiation patterns in the E- and H-planes, as well as the results for the impedance match, are presented in the paper.

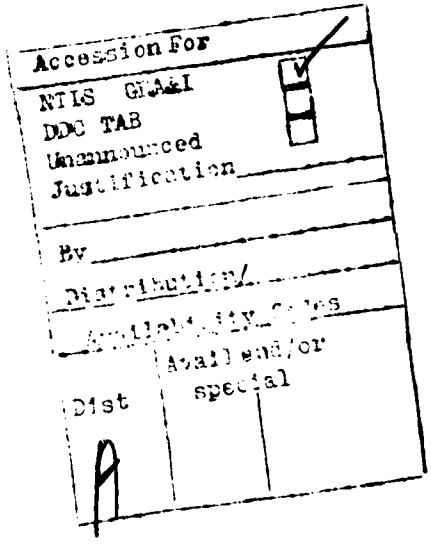

TABLE OF CONTENTS

LIST OF FIGURES

LIST OF TABLES

I. Introduction

Rectangular waveguide array feeds for reflector antennas play an important role in the design of satellite communication systems. To make the radiation pattern more symmetric in the E- and H-planes of the feed, a beam equalizer is needed. The design used in this case is a septum placed across the mouth of the waveguide such that the aperture distribution is reshaped to satisfy the new boundary conditions imposed by the septum. Consequently, the H-plane radiation pattern is narrowed to approach the E-plane pattern, thereby achieving the beam equalizing effect. However, the introduction of such a septum creates an impedance mismatch problem for the feed. To alleviate this problem, a matching post is placed behind the septum so that the reflection back into the waveguide is minimized.

The performance of this design over the desired frequency band is evaluated using a spectral domain approach, or more specifically, Galerkin's method applied in the spectral domain [1]. The scattered fields on both sides of the beam equalizer are represented in terms of their Fourier transforms or spectra which can be related to the induced surface currents on the septum and the post. These unknown induced currents are expanded in terms of known basis functions and unknown coefficients. A matrix equation for the unknown coefficients is derived by applying the boundary conditions, and the moment method is then employed in the spectral domain to solve for these unknown coefficients, which in turn give the answer to the unknown scattered fields. The scattered fields for all modes obtained in this manner are then used to compute the reflection and transmission coefficients for each mode, propagating or attenuated. A tacit assumption made is that the scattered field on the open-ended side of the waveguide is the same as

that in an infinitely long waveguide containing the beam equalizer. In other words, the truncation effects of the waveguide are ignored in this analysis. The transmission coefficients are used to weight the radiation field due to each mode of waveguide and the superimposed radiation pattern is computed. The reflection coefficients are used to assess the impedance matching performance. Numerical results indicate that the E- and H-plane principally polarized patterns are equalized extremely well over the entire frequency band of operation and that the impedance matching is also quite satisfactory.

II. Analysis

The geometry of the waveguide with septum and post is shown in Figure 1. Since the cross-section of the post is very small, the post is modeled as a narrow strip to simplify the analysis. The incident field is propagating in the z-direction towards the post as shown schematically in Figure 1. There are surface currents induced on the septum and the post due to the incident field. The scattered fields radiated by these induced surface currents then propagate in both the z-direction and the -z-direction, giving rise to the transmitted and the reflected waves, respectively. In the following analysis, the truncation effects of the waveguide at z=0 are ignored, as though the post and septum were located in an infinite guide.

The incident field in the waveguide can be expressed in terms of TE and TM modes in the usual manner:

TE_{nm} modes:

$$E_x^i = jh_{nm} \frac{\omega\mu(\frac{m\pi}{b})}{k_c^2} \cos(\frac{n\pi}{a}x) \sin(\frac{m\pi}{b}y) \exp(-j\beta_{nm}z)$$

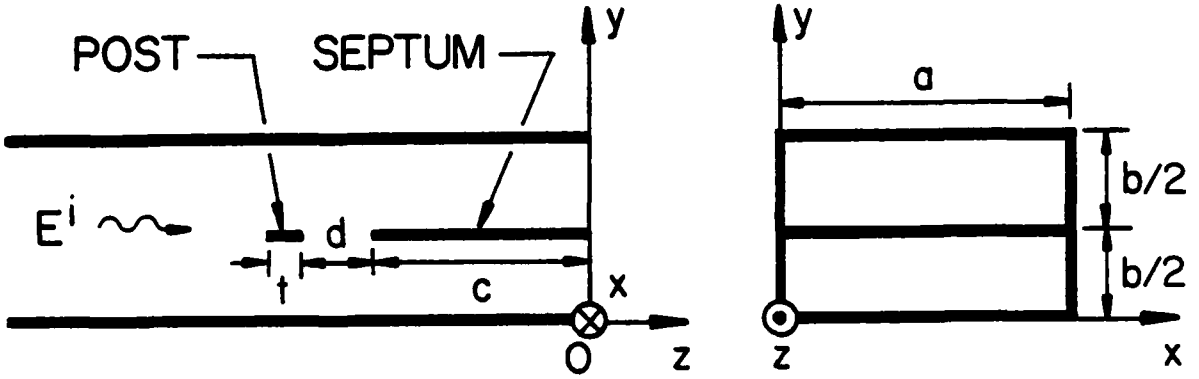

LONGITUDINAL-SECTION

CROSS-SECTION

$a = 1.3\ \lambda$

$b = 1.3\ \lambda$

$c = 0.25\ \lambda$

d IS VARIABLE

$t = 0.062\ \lambda$

$f = 3.95$ GHz

$\lambda = 0.076$ m

Figure 1. Geometry of the waveguide with septum and post.

$$E_y^i = -jh_{nm} Z_{TE} \frac{\beta_{nm}(\frac{n\pi}{a})}{k_c^2} \sin(\frac{n\pi}{a} x) \cos(\frac{m\pi}{b} y) \exp(-j\beta_{nm} z)$$

$$E_z^i = 0$$

$$H_x^i = -E_y^i / Z_{TE}$$

$$H_y^i = E_x^i / Z_{TE}$$

$$H_z^i = h_{nm} \cos(\frac{n\pi}{a} x) \cos(\frac{m\pi}{b} y) \exp(-j\beta_{nm} z) \qquad (1a)$$

TM_{nm} modes:

$$E_x^i = -je_{nm} \frac{\beta_{nm}(\frac{n\pi}{a})}{k_c^2} \cos(\frac{n\pi}{a} x) \sin(\frac{m\pi}{b} y) \exp(-j\beta_{nm} z)$$

$$E_y^i = -j e_{nm} Z_{TM} \frac{\omega\varepsilon(\frac{m\pi}{b})}{k_c^2} \sin(\frac{n\pi}{a} x) \cos(\frac{m\pi}{b} y) \exp(-j\beta_{nm} z)$$

$$E_z^i = e_{nm} \sin(\frac{n\pi}{a} x) \sin(\frac{m\pi}{b} y) \exp(-j\beta_{nm} z)$$

$$H_x^i = -E_y^i / Z_{TM} \quad ; \quad H_y^i = E_x^i / Z_{TM} \quad ; \quad H_z^i = 0 \qquad (1b)$$

where $k_c^2 = (\frac{n\pi}{a})^2 + (\frac{m\pi}{b})^2$; $\beta^2_{nm} = k^2 - k_c^2$; $k^2 = \omega^2 \mu\varepsilon$

$Z_{TE} = \omega\mu/\beta_{nm}$; $Z_{TM} = \beta_{nm}/(\omega\varepsilon)$

The scattered fields can be expressed in terms of their Fourier spectra, which are in turn related to the Fourier spectra of the induced surface currents. The Fourier spectra of the induced surface currents

are then solved for by the moment method applied in the transformed, i.e., the spectral domain. Specifically, Galerkin's method is used in the present analysis — the same basis functions are used as testing functions in the moment method. Upon solving the spectra of the induced surface currents, the scattered fields can be obtained in a straightforward manner. The analytic details follow.

Corresponding to each incident mode, the scattered fields E_x^s and E_z^s can be represented in the following form:

$$\begin{bmatrix} E_x^s \ (b/2 < y < b) \\ E_x^s \ (0 < y < b/2) \end{bmatrix} = \cos\left(\frac{n\pi}{a} x\right) \int_{-\infty}^{\infty} f_n(\alpha) \begin{bmatrix} \sin[\gamma_n(b-y)] \\ \sin \gamma_n y \end{bmatrix} \exp(-j\alpha z)d\alpha, \tag{2}$$

$$\begin{bmatrix} E_z^s \ (b/2 < y < b) \\ E_z^s \ (0 < y < b/2) \end{bmatrix} = \sin\left(\frac{n\pi}{a} x\right) \int_{-\infty}^{\infty} g_n(\alpha) \begin{bmatrix} \sin[\gamma_n(b-y)] \\ \sin \gamma_n y \end{bmatrix} \exp(-j\alpha z)d\alpha$$

where

$$\gamma_n = [k^2 - (\frac{n\pi}{a})^2 - \alpha^2]^{1/2} \tag{3}$$

and $f_n(\alpha)$, $g_n(\alpha)$ are the unknown Fourier spectra to be determined. The expression for E_y^s is then obtained from the Maxwell's equation $\nabla \cdot \vec{E} = 0$, giving

$$\begin{bmatrix} E_y^s \ (b/2 < y < b) \\ E_y^s \ (0 < y < b/2) \end{bmatrix} = \sin\left(\frac{n\pi}{a} x\right) \int_{-\infty}^{\infty} h_n(\alpha) \begin{bmatrix} \cos[\gamma_n(b-y)] \\ -\cos \gamma_n y \end{bmatrix} \exp(-j\alpha z)d\alpha \tag{4}$$

with

$$h_n(\alpha) = \frac{(\frac{n\pi}{a})\ f_n(\alpha) + j\alpha\ g_n(\alpha)}{\gamma_n} \tag{5}$$

Now that we have $\vec{E}$, we can find $\vec{H}$ by using the curl-of-$\vec{E}$ Maxwell's equation. However, in anticipation of relating the H-field with the induced surface currents on the septum and the strip, only the x- and the z- components of the H-field are computed, giving

$$\begin{bmatrix} H_x^s\ (b/2 < y < b) \\ \\ H_x^s\ (0 < y < b/2) \end{bmatrix} = \frac{-1}{j\omega\mu} \sin(\frac{n\pi}{a} x) \int_{-\infty}^{\infty} \exp(-j\alpha z)$$

$$\begin{bmatrix} [-\gamma_n\ g_n(\alpha) + j\alpha\ h_n(\alpha)] \cos [\gamma_n(b-y)] \\ \\ [\gamma_n\ g_n(\alpha) - j\alpha\ h_n(\alpha)] \cos \gamma_n\ y \end{bmatrix} d\alpha$$

$$\begin{bmatrix} H_z^s\ (b/2 < y < b) \\ \\ H_z^s\ (0 < y < b/2) \end{bmatrix} = \frac{-1}{j\omega\mu} \cos(\frac{n\pi}{a} x) \int_{-\infty}^{\infty} \exp(-j\alpha z)$$

$$\begin{bmatrix} [\gamma_n\ f_n(\alpha) + (\frac{n\pi}{a})\ h_n(\alpha)] \cos [\gamma_n(b-y)] \\ \\ [-\gamma_n\ f_n(\alpha) - (\frac{n\pi}{a})\ h_n(\alpha)] \cos \gamma_n\ y \end{bmatrix} d\alpha \tag{6}$$

The induced currents on the septum and the strip can also be expressed in terms of Fourier spectra. For each incident mode, we have

$$\begin{bmatrix} J_z\ (x,y = b/2,\ z) \\ J_x\ (x,y = b/2,\ z) \end{bmatrix} = \begin{bmatrix} \sin(\frac{n\pi}{a}\, x) \int_{-\infty}^{\infty} j_z(\alpha)\ \exp(-j\alpha z)\ d\alpha \\ \cos(\frac{n\pi}{a}\, x) \int_{-\infty}^{\infty} j_x(\alpha)\ \exp(-j\alpha z)\ d\alpha \end{bmatrix} \tag{7}$$

where $j_z(\alpha)$ and $j_x(\alpha)$ are Fourier spectra of the induced surface currents to be related to the spectra of the scattered H-field. This relationship is obtained by enforcing boundary conditions on the septum and the strip and can be written as

$$\begin{bmatrix} -H_x\ (y = \lim_{\varepsilon\to 0}\ (b/2 + \varepsilon)) + H_x\ (y = \lim_{\varepsilon\to 0}\ (b/2 - \varepsilon)) \\ H_z\ (y = \lim_{\varepsilon\to 0}\ (b/2 + \varepsilon)) - H_z\ (y = \lim_{\varepsilon\to 0}\ (b/2 - \varepsilon)) \end{bmatrix} = \begin{bmatrix} J_z \\ J_x \end{bmatrix} \tag{8}$$

where ε is a positive quantity.

Substitution of (6) and (7) into (8) leads to the following algebraic equations:

$$\begin{bmatrix} \frac{-2}{j\omega\mu} \cos(\frac{\gamma_n b}{2})\ [\gamma_n\, g_n(\alpha) - j\alpha h_n(\alpha)] \\ \frac{-2}{j\omega\mu} \cos(\frac{\gamma_n b}{2})\ [\gamma_n\, f_n(\alpha) + (\frac{n\pi}{a})\, h_n(\alpha)] \end{bmatrix} = \begin{bmatrix} j_z(\alpha) \\ j_x(\alpha) \end{bmatrix} \tag{9}$$

Substituting $h_n(\alpha)$ from (5) into (9) and manipulating the resulting equations leads to the following matrix equation for $f_n(\alpha)$ and $g_n(\alpha)$ in terms of the transform domain currents $j_x(\alpha)$ and $j_z(\alpha)$.

$$\begin{bmatrix} -j\alpha\left(\frac{n\pi}{a}\right) & k^2 - \frac{n^2\pi^2}{a^2} \\ k^2 - \alpha^2 & j\alpha\left(\frac{n\pi}{a}\right) \end{bmatrix} \begin{bmatrix} f_n(\alpha) \\ g_n(\alpha) \end{bmatrix} = \frac{-j\omega\mu\gamma_n}{2\cos\left(\frac{\gamma_n b}{2}\right)} \begin{bmatrix} j_z(\alpha) \\ j_x(\alpha) \end{bmatrix} \tag{10}$$

An inversion of (10) gives

$$\begin{bmatrix} f_n(\alpha) \\ g_n(\alpha) \end{bmatrix} = \frac{-j\omega\mu}{2k^2\gamma_n\cos\left(\frac{\gamma_n b}{2}\right)} \begin{bmatrix} -j\alpha\left(\frac{n\pi}{a}\right) & k^2 - \frac{n^2\pi^2}{a^2} \\ k^2 - \alpha^2 & j\alpha\left(\frac{n\pi}{a}\right) \end{bmatrix} \begin{bmatrix} j_z(\alpha) \\ j_x(\alpha) \end{bmatrix} \tag{11}$$

If the Fourier transforms of the currents $j_z(\alpha)$ and $j_x(\alpha)$ are known, we can obtain $f_n(\alpha)$ and $g_n(\alpha)$ from (11). Subsequently, (2), (4) and (6) can be used to derive the scattered fields by substituting for $f_n(\alpha)$ and $g_n(\alpha)$ in those expressions. The remaining task is to solve for the transform currents $j_z(\alpha)$ and $j_x(\alpha)$, using the Galerkin's method applied in the transform domain.

First we express the corresponding space domain currents in terms of a linear combination of a set of suitable basis functions with unknown coefficients.

$$\begin{bmatrix} J_x(x,z) \\ J_z(x,z) \end{bmatrix} = \begin{bmatrix} \cos\left(\frac{n\pi}{a}x\right) \left[U_c \sum_{i=1}^{I} A_i p_i(z) + U_t A_0 p_0(z)\right] \\ \sin\left(\frac{n\pi}{a}x\right) \left[U_c \sum_{\ell=1}^{L} B_\ell q_\ell(z)\right] \end{bmatrix}$$

$$= \begin{bmatrix} \cos\left(\frac{n\pi}{a}x\right) J_x(z) \\ \sin\left(\frac{n\pi}{a}x\right) J_z(z) \end{bmatrix} \tag{12}$$

where U_c and U_t are truncation functions on the septum and the strip, respectively,

$$U_c = \begin{cases} 1 & -c<z<0, \\ 0 & \text{otherwise} \end{cases}$$

$$U_t = \begin{cases} 1 & -(c+d+t)<z<-(c+d) \\ 0 & \text{otherwise} \end{cases}$$

Since the post is assumed to be of very small radius, we model it as a strip of width t, which is also small. Hence, only the x-directed current on the strip is expected to be significant. In (12), the unknowns to be evaluated are the coefficients A's and B's. From (7) and (12) it can be seen that

$$\begin{bmatrix} j_x(\alpha) \\ j_z(\alpha) \end{bmatrix} = \begin{bmatrix} \sum_{i=0}^{I} A_i P_i(\alpha) \\ \sum_{\ell=1}^{L} B_\ell Q_\ell(\alpha) \end{bmatrix} \tag{13}$$

where

$$P_i(\alpha) = \frac{1}{2\pi} \int_{-c}^{0} p_i(z) \exp(j\alpha z)\, dz, \qquad i = 1, 2, \ldots, I$$

$$P_0(\alpha) = \frac{1}{2\pi} \int_{-(c+d+t)}^{-(c+d)} p_0(z) \exp(j\alpha z)\, dz$$

$$Q_\ell(\alpha) = \frac{1}{2\pi}\int_{-c}^{0} q_\ell(z)\,\exp(j\alpha z)\,dz,\quad \ell = 1, 2, \ldots, L \tag{14}$$

Replacing (13) in (11), one obtains the expressions for the transform domain functions $f_n(\alpha)$ and $G_n(\alpha)$:

$$\begin{bmatrix} f_n(\alpha) \\ g_n(\alpha) \end{bmatrix} = \frac{-j\omega\mu}{2k^2\gamma_n \cos\left(\frac{\gamma_n b}{2}\right)} \begin{bmatrix} \left(k^2 - \frac{n^2\pi^2}{a^2}\right)\left(\sum_{i=0}^{I} A_i P_i(\alpha)\right) - j\alpha\frac{n\pi}{a}\left(\sum_{\ell=1}^{L} B_\ell Q_\ell(\alpha)\right) \\ j\alpha\frac{n\pi}{a}\left(\sum_{i=1}^{I} A_i P_i(\alpha)\right) + (k^2-\alpha^2)\left(\sum_{\ell=1}^{L} B_\ell Q_\ell(\alpha)\right) \end{bmatrix} \tag{15}$$

Substituting these expressions in (2), (4) and (6) we obtain the final results for the scattered fields in terms of the unknown coefficients A's and B's. In order to find these unknown coefficients, we enforce the boundary condition for the electric field on the septum and the strip, which requires the total tangential component of the electric field to be zero, i.e.,

$$\begin{bmatrix} E_x^s \\ E_z^s \end{bmatrix} = \begin{bmatrix} -E_x^i \\ -E_z^i \end{bmatrix} \quad \text{at } y = \frac{b}{2} \tag{16}$$

Using (1), (2), and (15) in (16) we derive the following equations for A's and B's.

$$\left[k^2 - \left(\frac{n\pi}{a}\right)^2\right]\sum_{i=0}^{I} A_i \int_{-\infty}^{\infty} \frac{1}{\gamma_n}\tan\left(\frac{\gamma_n b}{2}\right) P_i(\alpha)\,\exp(-j\alpha z)\,d\alpha$$

$$-j\frac{n\pi}{a}\sum_{\ell=1}^{L} B_\ell \int_{-\infty}^{\infty} \frac{\alpha}{\gamma_n}\tan\left(\frac{\gamma_n b}{2}\right) Q_\ell(\alpha)\,\exp(-j\alpha z)\,d\alpha$$

$$= \begin{cases} \dfrac{-2\,\frac{n\pi}{a}\,\beta_{nm}}{\omega\mu}\ \dfrac{k^2}{k_c^2}\ e_{nm}\sin(\frac{m\pi}{2})\ \exp\ (\mp j\beta_{nm}z), & \text{for TM modes.} \\ 2\,\frac{m\pi}{b}\ \dfrac{k^2}{k_c^2}\ h_{nm}\ \sin(\frac{m\pi}{2})\ \exp\ (\mp j\beta_{nm}z), & \text{for TE modes.} \end{cases}$$

$$j\,\frac{n\pi}{a}\sum_{i=0}^{I} A_i \int_{-\infty}^{\infty} \frac{\alpha}{\gamma_n}\ \tan\ (\frac{\gamma_n b}{2})\ P_i(\alpha)\ \exp\ (-j\alpha z)\ d\alpha$$

$$+ \sum_{\ell=1}^{L} B_\ell \int_{-\infty}^{\infty} \frac{(k^2-\alpha^2)}{\gamma_n}\ \tan\ (\frac{\gamma_n b}{2}) Q_\ell(\alpha)\ \exp\ (-j\alpha z)\ d\alpha$$

$$= \begin{cases} \mp \dfrac{2jk^2}{\omega\mu}\ e_{nm}\ \sin\ (\frac{m\pi}{2})\ \exp\ (\mp j\beta_{nm}z), & \text{for TM modes} \\ 0 & \text{, for TE modes} \end{cases} \qquad (17)$$

Now multiply both sides of (17) by the basis functions $p_i(z)$ and $q_\ell(z)$ and integrate over z to obtain the following equations.

$$(k^2 - \frac{n^2\pi^2}{a^2}) \sum_{i=0}^{I} A_i \int_{-\infty}^{\infty} \frac{1}{\gamma_n}\ \tan\ (\frac{\gamma_n b}{2})\ P_i(\alpha)\ P_i^*,(\alpha)\ d\alpha$$

$$- j\,\frac{n\pi}{a} \sum_{\ell=1}^{L} B_\ell \int_{-\infty}^{\infty} \frac{\alpha}{\gamma_n}\ \tan\ (\frac{\gamma_n b}{2})\ Q_\ell(\alpha)\ P_i^*,(\alpha)\ d\alpha$$

$$= \begin{cases} \dfrac{-2(\frac{n\pi}{a})\beta_{nm}}{\omega\mu} \dfrac{k^2}{k_c^2} e_{nm} \sin\dfrac{m\pi}{2} \begin{bmatrix} P_i^*, (\beta_{nm}) \\ P_{i'}, (\beta_{nm}) \end{bmatrix} & , i'=0,1,..,I \text{ for TM modes} \\ 2(\dfrac{m\pi}{b}) \dfrac{k^2}{k_c^2} h_{nm} \sin\dfrac{m\pi}{2} \begin{bmatrix} P_i^*, (\beta_{nm}) \\ P_{i'}, (\beta_{nm}) \end{bmatrix} & , i'=0,1,..,I \text{ for TE modes} \end{cases}$$

$$j\frac{n\pi}{a} \sum_{i=0}^{I} A_i \int_{-\infty}^{\infty} \frac{\alpha}{\gamma_n} \tan(\gamma_n \frac{b}{2}) P_i(\alpha) Q_\ell^*,(\alpha)\, d\alpha$$

$$+ \sum_{\ell=1}^{L} B_\ell \int_{-\infty}^{\infty} \frac{(k^2-\alpha^2)}{\gamma_n} \tan(\frac{\gamma_n b}{2}) Q_\ell(\alpha) Q_\ell^*,(\alpha)\, d\alpha$$

$$= \begin{cases} \begin{bmatrix} - \\ + \end{bmatrix} \dfrac{2jk^2}{\omega\mu} e_{nm} \sin\dfrac{m\pi}{2} \begin{bmatrix} Q_\ell^*, (\beta_{nm}) \\ Q_\ell, (\beta_{nm}) \end{bmatrix} & , \ell'=1,2,\ldots,L \text{ for TM modes} \\ 0 & , \ell'=1,2,\ldots,L \text{ for TE modes} \end{cases} \qquad (18)$$

The upper quantities within the square bracket in (18) are associated with positive z incident modes, and the lower quantities are associated with negative z incident modes. Both cases are included because we are interested in the transmission coefficients as well as the reflection coefficients. The integrals are evaluated by numerical integration, and the resulting system of linear equations is solved as usual for the unknowns A's and B's by matrix inversion.

The choice of basis functions, i.e., the p's and q's, is based on previous experience and the consideration of the behavior of the currents at the edges of the septum and the strip. Only two terms for the expansion of the currents on the septum are retained, which are believed to be adequate for this analysis. The basis functions and their Fourier transforms are shown in Table 1.

Let us now consider the case of interest, namely, one in which the incident fields are TE_{0m} modes. We have n=0, and the following relations:

$$\gamma_0^2 = k^2 - \alpha^2 \tag{19}$$

$$\beta_{0m}^2 = k^2 - \left(\frac{m\pi}{b}\right)^2 \tag{20}$$

When n=0, (18) can be simplified to the following

$$\sum_{i=0}^{2} A_i \int_{-\infty}^{\infty} \frac{\tan\left(\frac{\gamma_0 b}{2}\right)}{\frac{\gamma_0 b}{2}} P_i(\alpha)\, P_{i'}^*(\alpha)\, d\alpha$$

$$= \frac{4}{m\pi} \sin\left(\frac{m\pi}{2}\right) h_{0m} \begin{bmatrix} P_{i'}^*, (\beta_{0m}) \\ P_{i'}, (\beta_{0m}) \end{bmatrix}, \quad i'=0,\ 1,\ 2$$

$$\sum_{\ell=1}^{2} B_\ell \int_{-\infty}^{\infty} \gamma_0 \tan\left(\frac{\gamma_0 b}{2}\right) Q_\ell(\alpha)\, Q_{\ell'}^*(\alpha)\, d\alpha = 0, \quad \ell'=1,2 \tag{21}$$

The equations for A's and B's are uncoupled. Therefore, A's and B's can be solved for separately. The system of equations for B's is homogeneous,

Table 1. BASIS FUNCTIONS IN SPATIAL AND SPECTRAL DOMAINS

Spatial Domain	Spectral Domain
$p_0(z) = \exp\left[-\left(\frac{z+c+d+\frac{t}{2}}{\frac{t}{2}}\right)^2\right]$	$P_0(\alpha) = \frac{t}{4\sqrt{\pi}} \exp\left[-j\alpha\left(c+d+\frac{t}{2}\right)\right] \exp\left[-\left(\frac{t\alpha}{4}\right)^2\right]$
$p_1(z) = \frac{1}{\sqrt{1-\left(\frac{z+c/2}{c/2}\right)^2}}$	$P_1(\alpha) = \frac{c}{4} \exp\left(-j\alpha\frac{c}{2}\right) J_0\left(\frac{c\alpha}{2}\right)$
$p_2(z) = \frac{\frac{z+c/2}{c/2}}{\sqrt{1-\left(\frac{z+c/2}{c/2}\right)^2}}$	$P_2(\alpha) = \frac{jc}{4} \exp\left(-j\frac{\alpha c}{2}\right) J_1\left(\frac{c\alpha}{2}\right)$
$q_1(z) = \sqrt{1-\left(\frac{z+c/2}{c/2}\right)^2}$	$Q_1(\alpha) = \frac{c}{4} \exp\left(-j\frac{c\alpha}{2}\right) \frac{J_1\left(\frac{c\alpha}{2}\right)}{\frac{c\alpha}{2}}$
$q_2(z) = \frac{z+c/2}{c/2} \sqrt{1-\left(\frac{z+c/2}{c/2}\right)^2}$	$Q_2(\alpha) = \frac{jc}{4} \exp\left(-j\frac{c\alpha}{2}\right) \frac{J_2\left(\frac{c\alpha}{2}\right)}{\frac{c\alpha}{2}}$

J_0, J_1, and J_2 are Bessel functions of the first kind and of order zero, one, and two, correspondingly.

which leads to the conclusion that all B's are zero. Consequently, there are no components of the current in the z direction either in the septum or the strip. In the following development, only the system of equations for A's is investigated. Observe that the solution of A's involves an inversion of a 3 x 3 matrix, which is an easy task for the computer. However, the evaluation of the matrix elements involves nine complex integrals to be numerically integrated. Since there are singularities in these integrals, we must examine the integrands carefully to make sure that the numerical integration is applied correctly to give accurate results in spite of the singularities. Therefore, it is useful to write the expressions appearing in the integrands of (21) in an explicit manner as follows:

$$P_0P_0^* = \frac{t^2}{16\pi} \exp\left[-2\left(\frac{t\alpha}{4}\right)^2\right]$$

$$P_1P_0^* = \frac{ct}{16\sqrt{\pi}} J_0\left(\frac{c\alpha}{2}\right) \exp\left[-\left(\frac{t\alpha}{4}\right)^2\right] \exp\left[j\alpha\left(\frac{c}{2} + d + \frac{t}{2}\right)\right]$$

$$P_0P_1^* = \frac{ct}{16\sqrt{\pi}} J_0\left(\frac{c\alpha}{2}\right) \exp\left[-\left(\frac{t\alpha}{4}\right)^2\right] \exp\left[-j\alpha\left(\frac{c}{2} + d + \frac{t}{2}\right)\right]$$

$$P_2P_0^* = j\frac{ct}{16\sqrt{\pi}} J_1\left(\frac{c\alpha}{2}\right) \exp\left[-\left(\frac{t\alpha}{4}\right)^2\right] \exp\left[j\alpha\left(\frac{c}{2} + d + \frac{t}{2}\right)\right]$$

$$P_0P_2^* = -j\frac{ct}{16\sqrt{\pi}} J_1\left(\frac{c\alpha}{2}\right) \exp\left[-\left(\frac{t\alpha}{4}\right)^2\right] \exp\left[-j\alpha\left(\frac{c}{2} + d + \frac{t}{2}\right)\right]$$

$$P_1P_1^* = \frac{c^2}{16} J_0^2\left(\frac{c\alpha}{2}\right)$$

$$P_2P_2^* = \frac{c^2}{16} J_1^2\left(\frac{c\alpha}{2}\right) \qquad (22)$$

Note that $P_1P_2^*$, $P_2P_1^*$, etc. are not of interest here because the corresponding integrands are odd and therefore the integrals involving them are identically zero. Now observe that the integrand in (21) contains a simple pole located at $\alpha = \beta_{01}$ on the path of integration for $0 < \alpha < \infty$, provided that the wave number satisfies the following condition:

$$\frac{\pi}{b} < k < 3\frac{\pi}{b} \tag{23}$$

This is the case when the incident field is the dominant, propagating mode in the waveguide. Introduction of some loss in the medium clarifies the position of the poles along the integration path, as shown in Fig. 2. Each of the integrals in (21) can be written in the following form

$$\int_{-\infty}^{\infty} F(\alpha)d\alpha = \int_{-\infty}^{-\beta_{01}} F(\alpha)d\alpha + \int_{-\beta_{01}}^{\beta_{01}} F(\alpha)d\alpha + \int_{\beta_{01}}^{\infty} F(\alpha)d\alpha + \pi j \text{ Res } (-\beta_{01})$$

$$- \pi j \text{ Res } (\beta_{01}) = \int_{-\infty}^{-2\beta_{01}} F(\alpha)d\alpha + \int_{-2\beta_{01}}^{0} F(\alpha)d\alpha$$

$$+ \int_{0}^{2\beta_{01}} F(\alpha)d\alpha + \int_{2\beta_{01}}^{\infty} F(\alpha)d\alpha + \pi j \text{ Res } (-\beta_{01}) - \pi j \text{ Res } (\beta_{01})$$

$$= \int_{-\infty}^{-2\beta_{01}} F(\alpha)d\alpha + \int_{-\beta_{01}}^{0} [F(-2\beta_{01} - \alpha) + F(\alpha)]\, d\alpha$$

$$+ \int_{0}^{\beta_{01}} [F(\alpha) + F(2\beta_{01} - \alpha)]\, d\alpha$$

$$+ \int_{2\beta_{01}}^{\infty} F(\alpha)d\alpha + \pi j \text{ Res } (-\beta_{01}) - \pi j \text{ Res } (\beta_{01}) \tag{24}$$

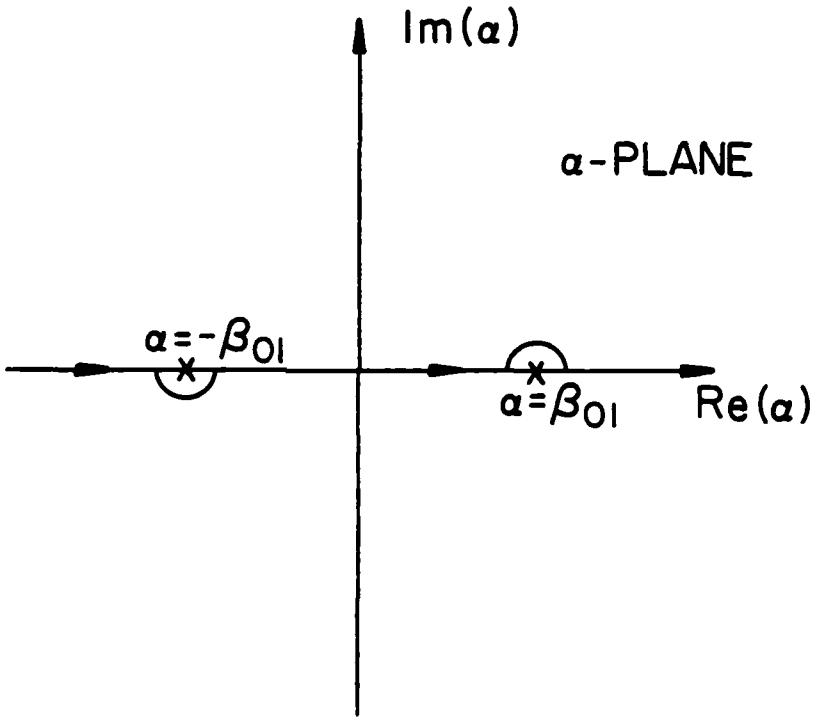

Figure 2. Location of poles in the integration path of integrals in Eq. (21).

In the above equation, a bar across the integral sign means principal value integration. The method of foldover as shown makes the new integrand remain bounded at the singularity of the old integrand; hence, this new integral is easily evaluated by the numerical method. Also, since the integrand goes to zero rapidly as α becomes large, the integration limit ∞ can be replaced by a large number, e.g., 14 β_{01}. It should be noted that if the foldover method was not used, the integral could still be evaluated numerically, in some cases, but the integration limit ∞ must be replaced by a much larger number which requires increased computer time and the results are less accurate. The residues given in (24) are easily calculated and are given by the general form

$$\text{Res}(\pm\beta_{01}) = \frac{4}{b^2(\pm\beta_{01})} \; P_i(\alpha)\, P^*_{i'}(\alpha) \Big|_{\alpha = \pm\beta_{01}}, \quad i, i' = 0, 1, 2$$

with $P_i(\alpha)\, P^*_{i'}(\alpha)$ given in (22).

(25)

Having discussed the evaluation of the matrix elements in detail, we can proceed to solve the matrix equation (21) to obtain the A's. Having found these A's, we compute $f_0(\alpha)$ from (15) and then calculate the scattered fields from (2). For n=0, both E^s_z and $E^s_y = 0$, and there is only E^s_x, which can be written as

$$\begin{bmatrix} E^s_x \left(\frac{b}{2} < y < b\right) \\ E^s_x \left(0 < y < \frac{b}{2}\right) \end{bmatrix} = \int_{-\infty}^{\infty} \frac{-j\omega\mu_0}{2\gamma_0 \cos\left(\frac{\gamma_0 b}{2}\right)} \begin{bmatrix} \sum_{i=0}^{2} A_i P_i(\alpha) \end{bmatrix} \begin{bmatrix} \sin[\gamma_0 (b-y)] \\ \sin \gamma_0 y \end{bmatrix}$$

$$\exp(-j\alpha z)\, d\alpha \qquad (26)$$

$$\text{where } \gamma_0 = \begin{cases} \sqrt{k^2 - \alpha^2} & \text{if} \quad k > |\alpha| \\ j\sqrt{\alpha^2 - k^2} & \text{if} \quad k < |\alpha| \end{cases}$$

Let us evaluate (26) at $y = \frac{b}{2}$,

$$E_x^s(y=\frac{b}{2}) = \frac{-jkbZ_0}{4} \left[\sum_{i=0}^{2} A_i \int_{-\infty}^{\infty} \frac{\tan \frac{\gamma_0 b}{2}}{\frac{\gamma_0 b}{2}} P_i(\alpha) \exp(-j\alpha z)\, d\alpha \right] \tag{27}$$

Since the scattered fields on both sides of the beam equalizer are given by (27), we can compute the transmission and reflection coefficients by normalizing these scattered fields to the incident field given in (1). The reflection coefficient R can be expressed as

$$R = \left. \frac{E_x^s}{E_x^i} \right|_{\substack{y=\frac{b}{2} \\ z<0}}$$

$$= \frac{-\pi \exp(j\beta_{01} z)}{4\, h_{01}} \sum_{i=0}^{2} A_i \left[2\pi j \sum_{m=1,3,5,\ldots} \text{Res}_i(\zeta_m) \right] \tag{28}$$

where the poles are given by

$$\zeta_1 = -\beta_{01} = -\sqrt{k^2 - (\tfrac{\pi}{b})^2} \quad ; \qquad \zeta_{m \geq 3} = j\sqrt{(\tfrac{m\pi}{b})^2 - k^2}$$

and the residues at these poles are given by

$$\text{Res}_i(\zeta_1) = \frac{4\, P_i(-\beta_{01}) \exp(jz\beta_{01})}{b^2\, (-\beta_{01})}$$

$$\text{Res}_i(\zeta_m) = \text{Res}_i(j\chi_m) = \frac{4\, P_i(j\chi_m)\, \exp\,(\chi_m z)}{b^2(j\chi_m)} \quad , \qquad m \geq 3$$

with $\chi_m = \sqrt{(\frac{m\pi}{b})^2 - k^2}$

$$P_0(j\chi_m) = \frac{t}{4\sqrt{\pi}}\ \exp\,[\chi_m(c+d+\frac{t}{2})]\ \exp\,[(\frac{t\chi_m}{4})^2]$$

$$P_1(j\chi_m) = \frac{c}{4}\exp\,(\frac{\chi_m c}{2})\ I_0\ (\frac{c}{2}\chi_m)$$

$$P_2(j\chi_m) = \frac{jc}{4}\exp\,(\frac{\chi_m c}{2})\ jI_1\ (\frac{c}{2}\chi_m)$$

and I_0, I_1 are modified Bessel functions of the first kind. In deriving (28), the integral in (27) has been evaluated by the residue theorem with the contour closed in the upper half of the α-plane. By the same token, the transmission coefficient T can also be obtained, except this time the contour is closed in the lower half of the α-plane.

$$T = \frac{E_x^s}{E_x^i}\ \Bigg|\ \begin{matrix} y=\frac{b}{2} \\ z>0 \end{matrix}$$

$$= \frac{-\pi \exp(j\beta_{01}z)}{4h_{01}} \sum_{i=0}^{2} A_i \left[-2\pi j \sum_{m=1,3,5,\ldots} \text{Res}_i\ (\zeta_m)\right] \qquad (29)$$

where the poles are given by

$$\zeta_1 = \beta_{01} = \sqrt{k^2 - (\frac{\pi}{b})^2}$$

$$\zeta_{m\geq 3} = -j\sqrt{(\frac{m\pi}{b})^2 - k^2}$$

and the residues at these poles are given by

$$\text{Res}_i(\gamma_1) = \frac{4\, P_i(\beta_{01})\, \exp\,(-j\beta_{01} z)}{b^2 \beta_{01}}$$

$$\text{Res}_i(\gamma_m) = \text{Res}_i(-j\chi_m) = \frac{4\, P_i(-j\chi_m)\, \exp\,(-\chi_m z)}{b^2(-j\chi_m)} \quad , \quad m \geq 3$$

with $\chi_m = \sqrt{(\frac{m\pi}{b})^2 - k^2}$

$$P_0\,(-j\chi_m) = \frac{t}{4\sqrt{\pi}}\ \exp\,[-\chi_m(c+d+\frac{t}{2})]\ \exp\,[(\frac{t\chi_m}{4})^2]$$

$$P_1\,(-j\chi_m) = \frac{c}{4} \exp\,(-\frac{\chi_m c}{2})\ I_0\,(\frac{c}{2}\chi_m)$$

$$P_2\,(-j\chi_m) = \frac{jc}{4} \exp\,(-\chi_m \frac{c}{2})\ [-jI_1\,(\frac{c}{2}\chi_m)]$$

and I_0, I_1 are modified Bessel functions of the first kind. Numerical results indicate that minimum reflection and maximum transmission can be achieved if the separation between the septum and the strip is 0.1 wavelength for the given dimensions in Fig. 1.

The radiation pattern of the waveguide feed with beam equalizer can now be computed in the following manner. First, the aperture field distribution in the plane containing the waveguide mouth is estimated by a superposition of the waveguide mode field at this plane with each mode being weighted by the corresponding transmission coefficients for the modes. Since the transmission coefficients have been evaluated at a different reference plane, it is necessary to refer these transmission coefficients back to the aperture plane. This is done by multiplying the transmission

coefficients by an appropriate correcting factor, which is a phase factor for a propagating mode and is an exponential factor for an attenuated mode. The radiation pattern is then obtained by the familiar Fourier transform relation between the far field and the aperture field. For TE_{nm} modes, the far fields are given by the following expressions [2]:

$$E_\theta = -\left(\frac{\mu}{\varepsilon}\right)^{1/2} \frac{(\pi ab)^2 \sin\theta}{2\lambda^3 R\, k_{nm}^2} \left[1 + \frac{\beta_{nm}}{k}\cos\theta + R\left(1 - \frac{\beta_{nm}}{k}\cos\theta\right)\right]$$

$$\cdot \left[\left(\frac{n\pi}{a}\sin\phi\right)^2 - \left(\frac{m\pi}{b}\cos\phi\right)^2\right] \tilde{\psi}_{nm}(\theta,\phi)$$

$$E_\phi = -\left(\frac{\mu}{\varepsilon}\right)^{1/2} \frac{(\pi ab)^2 \sin\theta \sin\phi \cos\phi}{2\lambda^3 R}$$

$$\cdot \left[\cos\theta + \frac{\beta_{nm}}{k} + R\left(\cos\theta - \frac{\beta_{nm}}{k}\right)\right] \psi_{nm}(\theta,\phi) \qquad (30)$$

with

$$\psi_{nm}(\theta,\phi) = \left[\frac{\sin\left(\frac{\pi a}{\lambda}\sin\theta\cos\phi + \frac{n\pi}{2}\right)}{\left(\frac{\pi a}{\lambda}\sin\theta\cos\phi\right)^2 - \left(\frac{n\pi}{2}\right)^2}\right] \cdot \left[\frac{\sin\left(\frac{\pi b}{\lambda}\sin\theta\sin\phi + \frac{m\pi}{2}\right)}{\left(\frac{\pi b}{\lambda}\sin\theta\sin\phi\right)^2 - \left(\frac{m\pi}{2}\right)^2}\right]$$

$$\cdot \exp\left\{-j\left[kR - \frac{\pi}{\lambda}\sin\theta\,(a\cos\phi + b\sin\phi) - (n+m+1)\frac{\pi}{2}\right]\right\}$$

where (R,θ,ϕ) are the conventional right-handed spherical coordinates. The total radiation pattern is then obtained by a superposition of these individual mode patterns with the appropriate transmission coefficients referenced at the aperture plane. Computed patterns and measured results are presented in the next section.

III. Computed Results

The performance of the square waveguide feed with beam equalizer is evaluated over a frequency band of operation. The computed radiation patterns in the E- and H-planes are presented in Figure 3. The beam equalization is quite satisfactory over the entire band. The corresponding aperture field distributions are shown in Figure 4. Looking at these aperture distributions, one can explain how the beam equalizer works. It goes as follows. The aperture distribution for the E-plane pattern is uniform which gives a familiar $(\sin x)/x$ type pattern. The H-plane pattern is due to a cosine-taper type of aperture distribution if there is no beam equalizer present. Hence, the beamwidth is larger than that of the E-plane pattern for a square waveguide aperture. However, the introduction of the beam equalizer forces the H-plane aperture field to vanish at the center of the aperture, which makes the field distribution look more uniform. Hence, the main lobe of the H-plane pattern narrows to achieve the beam equalization effect in the E- and H-planes. The pattern is mainly determined by the septum; the post is present for impedance matching. The computed reflection coefficients over the frequency band are shown in Table 2.

IV. Conclusions

A septum and an impedance matching post used as a beam equalizer in an open-ended waveguide-feed for reflectors used in satellite communications systems have been analyzed by using a spectral domain approach. The computed radiation patterns in the E- and H-planes, as well as the impedance match results, have been presented in the paper. The performance

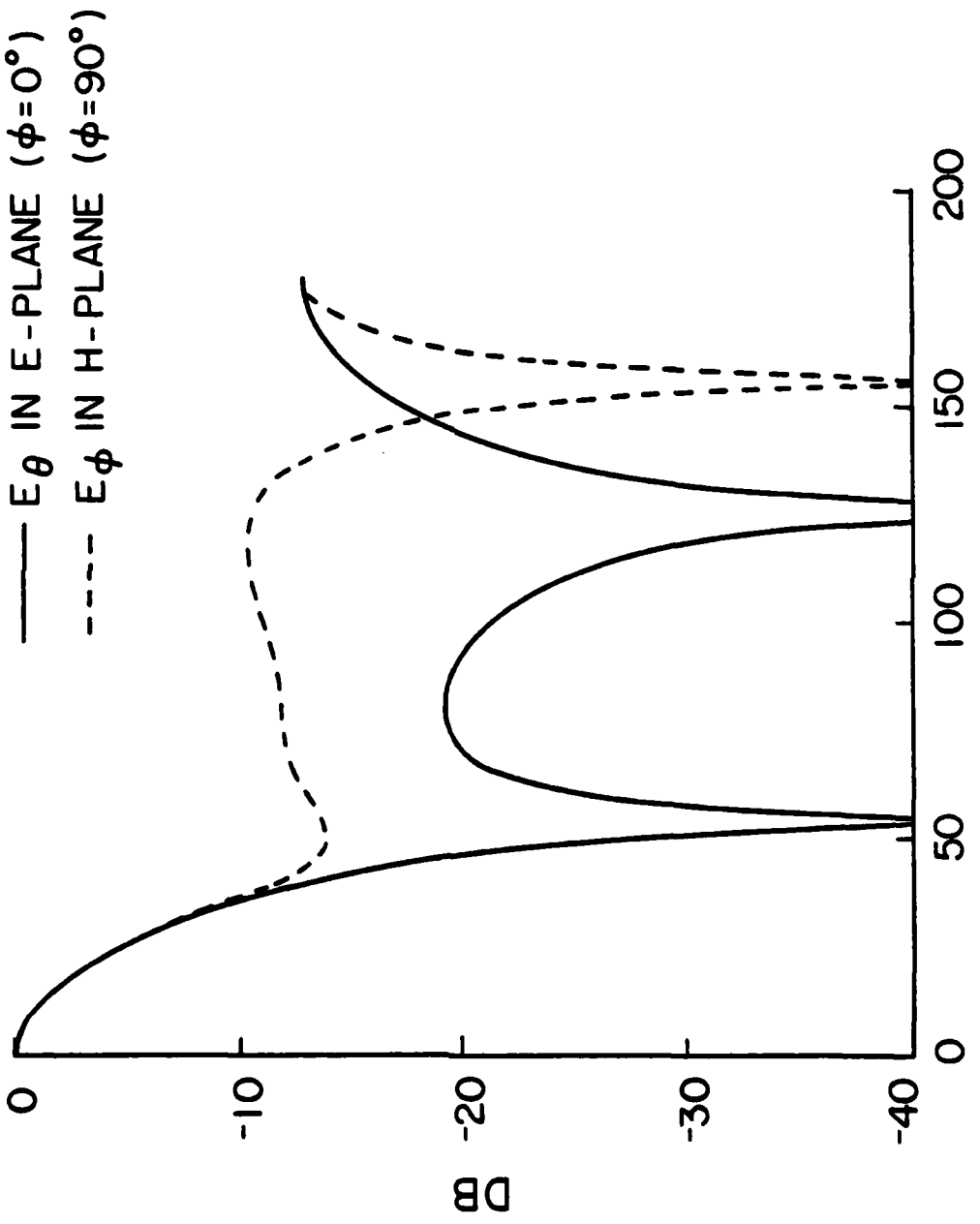

Figure 3(a). Radiation patterns in E- and H-planes at lower bandedge of a 10% center frequency band.

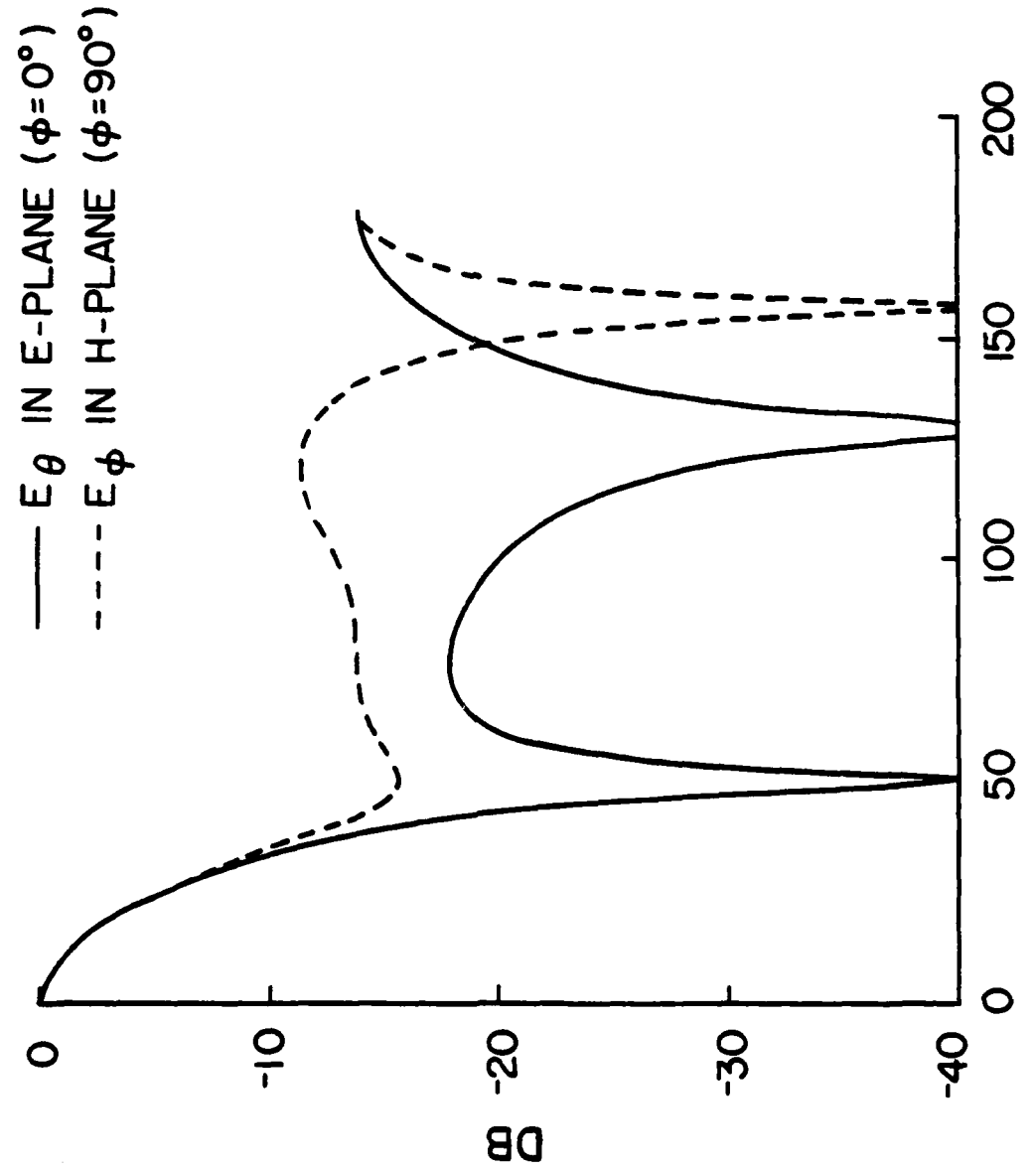

Figure 3(b). Radiation patterns in E- and H-planes at center frequency of a 10% center frequency band.

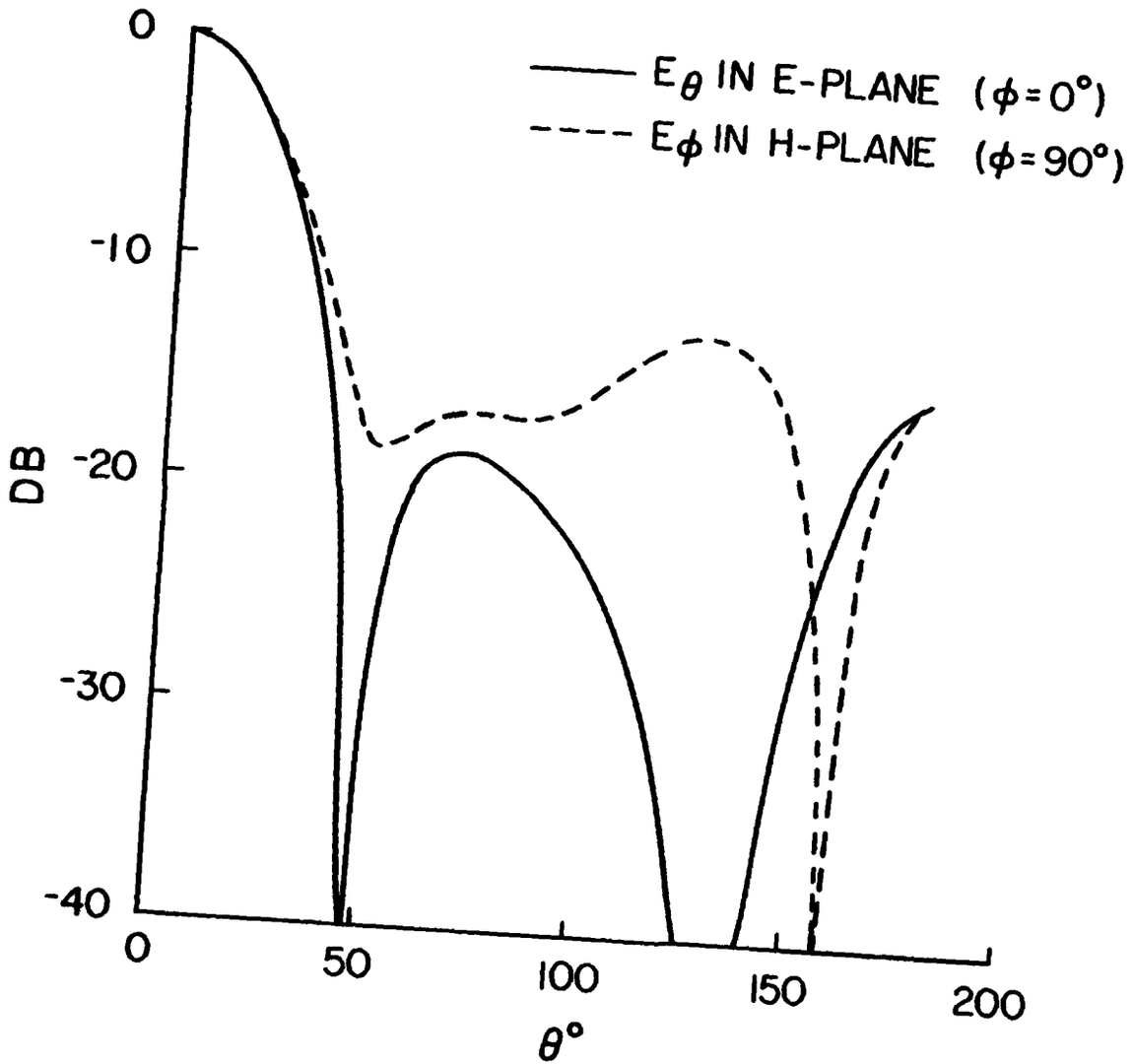

Figure 3(c). Radiation patterns in E- and H-planes at upper bandedge of a 10% center frequency band.

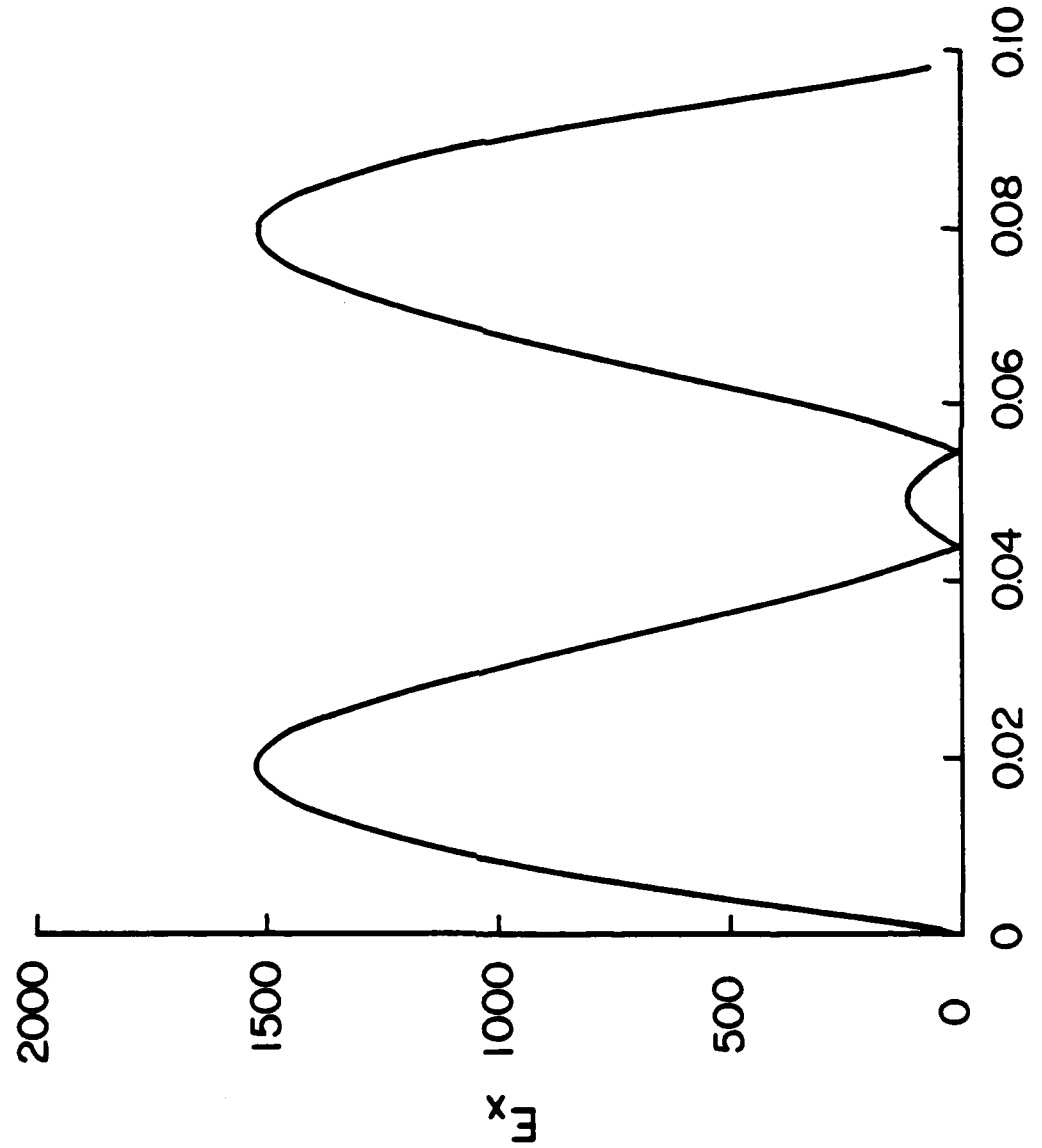

Figure 4(a). Aperture distribution at lower bandedge of a 10% center frequency band.

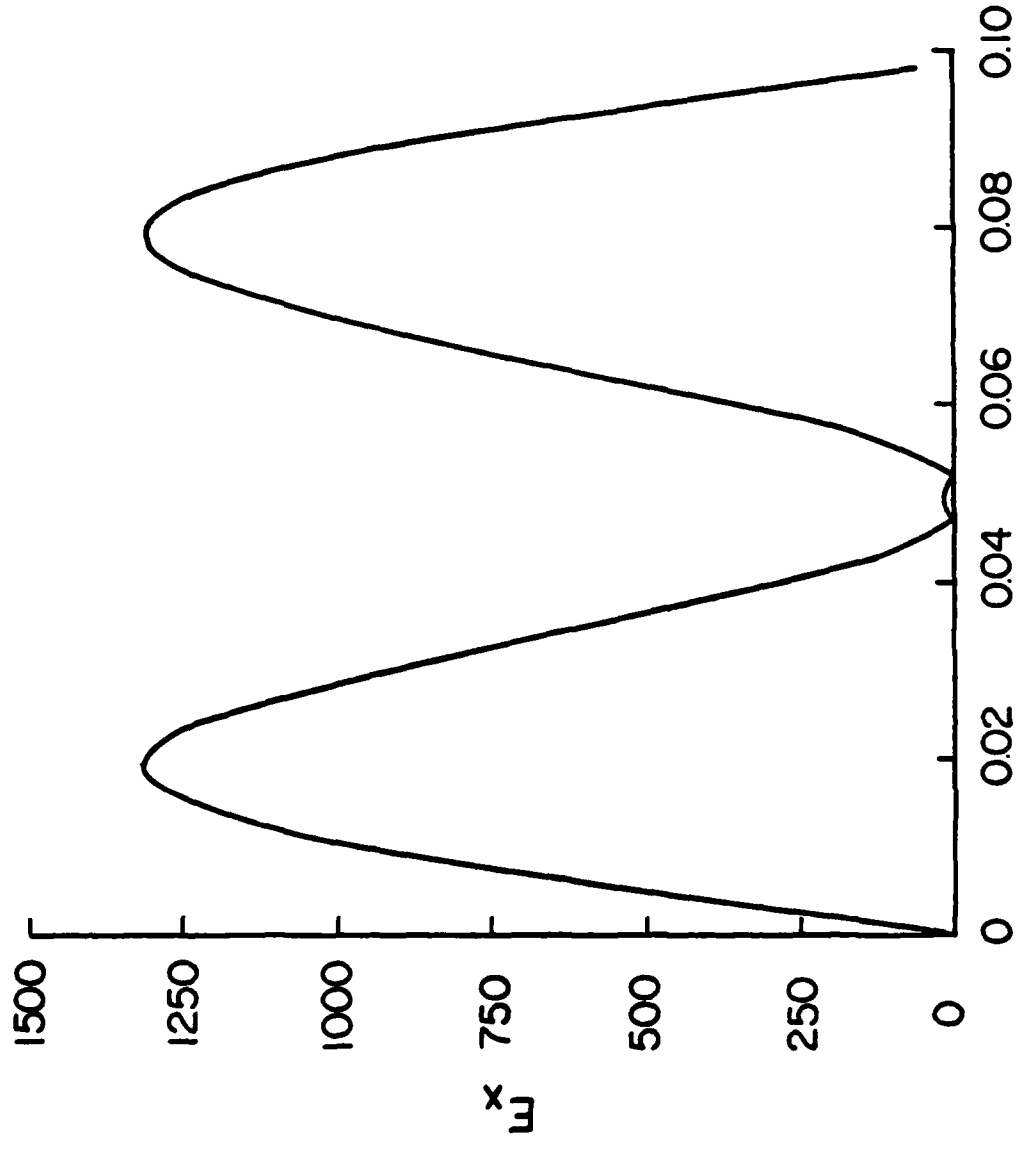

Figure 4(b). Aperture distribution at center frequency of a 10% center frequency band.

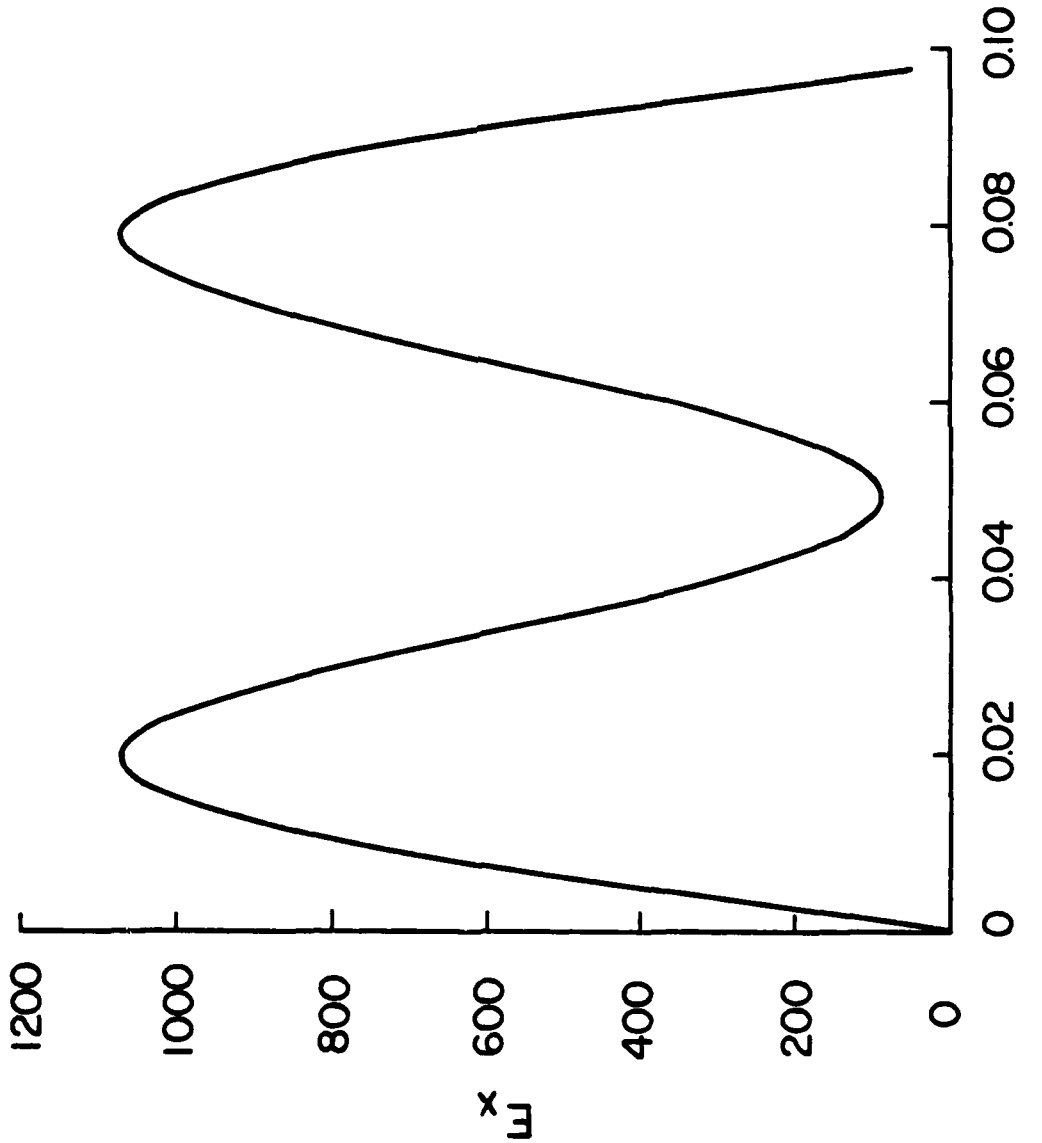

Figure 4(c). Aperture distribution at upper bandedge of a 10% center frequency band.

TABLE 2

REFLECTION COEFFICIENTS OVER THE FREQUENCY BAND

Frequency (GHz)	Reflection coefficient Γ	VSWR = $\frac{1+\lvert\Gamma\rvert}{1-\lvert\Gamma\rvert}$
3.75	$0.2729/\underline{-130.25}°$	1.751
3.85	$0.1879/\underline{-134.90}°$	1.463
3.95	$0.1071/\underline{-142.02}°$	1.240
4.05	$0.0358/\underline{-167.87}°$	1.074
4.15	$0.0442/\underline{73.10}°$	1.092

of the beam equalizer over the entire band of operating frequency has been evaluated. The results indicate that the E- and H-plane principally polarized patterns are equalized extremely well over the entire frequency band of operation and that the impedance matching is also satisfactory.

References

[1] R. Mittra and T. S. Li, "A spectral domain approach to the numerical solution of electromagnetic scattering problems," AEU, vol. 29, pp. 217-222, 1975.

[2] S. Silver, Microwave Antenna Theory and Design, M.I.T. Radiation Laboratory Series, McGraw-Hill Company, New York, 1949.